Copy No. 25

AEROBALLISTICS RANGE MEASUREMENTS OF THE PERFORMANCE AND STABILITY OF SUPERSONIC AIRCRAFT

by
H.R. Warren

DEFENCE RESEARCH BOARD

CANADIAN ARMAMENT RESEARCH AND DEVELOPMENT ESTABLISHMENT

Valcartier, Quebec December, 1958

NOTE

CARDE Technical Memoranda are prepared for the purpose of distributing information on technical subjects or interim reporting on unfinished projects. They may contain information which is tentative.

CARDE TECHNICAL MEMORANDUM AB-32 UNCLASSIFIED

P.C.C. D46-95-51-06

AEROBALLISTICS RANGE MEASUREMENTS OF THE PERFORMANCE AND STABILITY OF SUPERSONIC AIRCRAFT

H.R. Warren *

* The de Havilland Aircraft of Canada, Limited

CANADIAN ARMAMENT RESEARCH AND DEVELOPMENT ESTABLISHMENT

Valcartier, P.Q. December, 1958

SUMMARY

This paper describes a method of measuring aircraft drag and some stability characteristics in free flight. Tests have been made firing scale models of existing delta- and straight-winged aircraft in an aeroballistics range at supersonic speed and high Reynolds number. Histories of the model's speed, attitude and lateral motion during the flight have been obtained using light screens and yaw cards, while shock wave and flow behaviour were observed with schlieren systems. Either a longitudinal or a lateral type of motion during the flight could be obtained by suitable adjustment to the model's ballast and its position in the launching sabot. With the modes of flight thus separated, it was possible to devise quite simple methods of analysis to evaluate the stability derivatives.

With these methods, dynamic and static derivatives have been determined for both the lateral and longitudinal cases which compare well with values obtained in high speed wind tunnels and with large scale rocket launched free flight models. Extensions of the present technique, in terms of size and speed of the model, and development of instrumentation to obtain additional aerodynamic data are discussed.

C O N T E N T S

FIGURES

1.0 INTRODUCTION

The technique of obtaining aerodynamic information from aeroballistics range measurements has been used successfully at such establishments as the Canadian Armament Research and Development Establishment (CARDE) and the Ballistics Research Laboratories[1] for several years for missiles and ballistic projectiles. The accuracy of the results obtained and the inherent simplicity of the method have led, more recently, to the use of the range at CARDE for tests on a wider variety of shapes,[2,3] including delta wings, spheres and aeroplanes. The present report describes the progress that has been made with various aeroplane models in the aeroballistics range, including the AVRO CF-105, the Bell X-1 and a simple aspect-ratio 2 delta-winged aircraft.

The basic test equipment was that used at CARDE for testing missiles and ballistic shapes. The models were launched at supersonic speed from a 5.9" smooth-bore gun by means of a sabot carrier. The sabot was discarded at the entrance to the range and for the first four hundred feet of the model's flight down the range, measurements were taken with the aid of velocity-measuring light screens, schlieren photography and yaw cards. The latter, consisting of sheets of light paper mounted at $2\frac{1}{2}$', 5' and 10' intervals down the range, were punctured by the model in its free flight. By subsequent measurements of these cuts, the model's angles of pitch, roll and yaw, as well as the lateral displacement of its centre of gravity with respect to the line of fire could be determined.

Although some aeroplane tests have been carried out at BRL and at the NACA, [4] this was the first time an aeroballistics range had been used for a comprehensive program of tests on models of existing aircraft where direct comparison with results of other test methods could be made.

1.0 INTRODUCTION, (Cont'd...)

Some mention of the reasons for undertaking the study may therefore be of interest. With the present trend in aircraft design to thin, highly-loaded wings of short span and long thin fuselages, there is an increasing need for knowledge of dynamic characteristics, particularly cross-coupling effects, especially at an early stage in design. Accurate drag data is also essential in determining the performance of such aircraft. Alternative methods for obtaining this information heretofore have been by estimation, by wind tunnel tests[5] and by ground-launched, rocket-boosted free-flight models.[6,7]

Methods of estimation or calculation are subject to large errors because they are either based on an extrapolation to high Mach number of experimental low speed data or are based on theory alone. Also, even slight configurational differences from a similar aircraft could have a large effect on values of some of the derivatives, such as C_{n_p} and C_{l_r}.

Wind tunnel methods have been devised for measuring a few of the dynamic derivatives, and good accuracy has been obtained in the determination of $\left(C_{M_\alpha} + C_{M_q}\right)$, $\left(C_{L_\alpha} + C_{L_q}\right)$, and C_{l_p}. [8] The equipment used to oscillate the models and to analyse the results can be quite complicated and costly and the methods are unsuitable for the determination of cross-derivatives. The use of a free-flight technique eliminates the need for the sting support used in the wind tunnel and so avoids possible errors in correcting for this. This is particularly important in the measurement of aircraft drag. Tunnel wall corrections, which are difficult to allow for accurately, especially in transonic wind-tunnel tests, are also eliminated. As either aeroballistics range tests or ground-launched tests are done at or near sea-level density with full

1.0 INTRODUCTION, (Cont'd...)

scale Mach number, the Reynold's number is generally higher than with wind-tunnel tests. For the CARDE tests at Mach 2.6 described here, the Reynold's number was 4.7 million based on mean aerodynamic chord.

The greatest advantage of the free flight tests is the ability to observe the complete three-dimensional dynamic behaviour of the model over a wide range of Mach numbers extending into the low hypersonic range with no restrictions applied to it. The method of ground-launched model testing using ground tracking equipment and telemetry to record test data is a well-proven technique from which most of the necessary test information can be obtained. Its chief drawback is that because of the size and complexity of the model and the amount of preparation and cost necessary for each test, it does not lend itself either to a quick appraisal of a number of different configurations or to a long program of numerous tests on a single configuration.

It is because of the need for such a quick appraisal in early design work or a full program to complete a final design evaluation, that the two main advantages of the range technique over the ground-launched method are important. These are the simplicity of the instrumentation and the small size and cheapness of the model itself. Because measurements are made externally, the model carries no instrumentation, but requires only to be dimensionally accurate and suitably ballasted. The basic instrumentation required in the aeroballistics range is identical to that used for missile and projectile testing and provides a much cheaper and quicker means of obtaining dynamic information or drag data than by the use of airborne telemetry with large scale ground-to-air models.

1.0 INTRODUCTION, (Cont'd...)

With these considerations in view the program was initiated with the following successive objectives:

(a) to develop manufacturing methods which ensured the necessary standard of accuracy within a reasonable cost per model.

(b) to adapt techniques of model metrology to suit this application.

(c) to achieve a satisfactory launch and obtain useful and accurate test records.

(d) to devise methods of analysis to extract the required aerodynamic information from the records.

This report describes the progress that has been made at CARDE in meeting these objectives. Although much further development work can be done particularly with regard to the analysis methods, the results to date indicate that the aeroballistics range method can prove a useful complement to the wind-tunnel in providing data on dynamic stability and drag not otherwise available and in checking static stability parameters obtained in the wind tunnel. The ability to make rapid changes in configuration and to check their effects on drag and flight dynamics would be particularly valuable in the preliminary testing of an aeroplane design, early enough in its development that such configurational changes could still be made.

2.0 NOTATION

2.1 Model and Test Characteristics

a	Speed of Sound	ft./sec.
b	Model Wing Span	ft.
$\bar{c}$	Wing Mean Aerodynamic Chord	ft.
g	Acceleration due to Gravity = 32.2	ft./sec.^{2}
I_x	Moment of Inertia about longitudinal or roll reference axis	slug ft.^{2}
I_y	Moment of Inertia about lateral or pitch reference axis	slug ft.^{2}
I_z	Moment of Inertia about vertical or yaw axis	slug ft.^{2}
I_{xz}	Product of Inertia (Note that $I_{xy} = I_{yz} = 0$ because of symmetry)	slug ft.^{2}
M	Mach Number = $\frac{V}{a}$	
p	Static Air Pressure	lb./sq.ft.
q	Dynamic Air Pressure = $\frac{\rho}{2} V^2 = 0.7\ pM^2$	lb./sq.ft.
R_{50}	Retardation of Model	ft./sec./50ft. of flight
S	Wing Area	sq.ft.
V	Forward Velocity	ft./sec.
W	Model Weight	lb.
$Y_{c.g.}$	Position of Model Centre of Gravity laterally from the line of fire (positive to the right)	ft.
$Z_{c.g.}$	Position of Model Centre of Gravity below the line of fire	ft.
ε	Inclination of Principal Longitudinal Axis of Inertia below reference longitudinal axis	deg.
ρ	Air Density	slug/cu.ft.

2.2 Aerodynamic Characteristics

$$C_D = \frac{\text{Drag Force}}{1/2\ \rho\ V^2\ S}$$

$$C_L = \frac{\text{Lift Force}}{1/2\ \rho\ V^2\ S}$$

$$C_{L_\alpha} = \frac{\partial C_L}{\partial \alpha}$$

$$C_l = \frac{\text{Rolling Moment}}{1/2\ \rho\ V^2\ S\ b}$$

$$C_{l_\beta} = \frac{\partial C_l}{\partial \beta}$$

$$C_{l_p} = \frac{\partial C_l}{\partial \frac{p\ b}{2V}}$$

$$C_{l_r} = \frac{\partial C_l}{\partial \frac{r\ b}{2V}}$$

$$C_m = \frac{\text{Pitching Moment}}{1/2\ \rho\ V^2\ S\ \bar{c}}$$

$$C_{m_\alpha} = \frac{\partial C_m}{\partial \alpha}$$

$$C_{m_{\dot{\alpha}}} = \frac{\partial C_m}{\partial \frac{\dot{\alpha}\bar{c}}{2V}}$$

$$C_{m_q} = \frac{\partial C_m}{\partial \frac{q\ \bar{c}}{2V}}$$

$$C_n = \frac{\text{Yawing Moment}}{1/2\ \rho\ V^2\ S\ b}$$

$$C_{n_\beta} = \frac{\partial C_n}{\partial \beta}$$

$$C_{n_p} = \frac{\partial C_n}{\partial \frac{p\ b}{2V}}$$

$$C_{n_r} = \frac{\partial C_n}{\partial \frac{r\ b}{2V}}$$

$$C_y = \frac{\text{Side Force}}{1/2\ \rho\ V^2\ S}$$

$$C_{y_\beta} = \frac{\partial C_y}{\partial\ \beta}$$

2.2 Aerodynamic Characteristics (Cont'd.)

K	Damping factor of model oscillation	per second
p	Rate of Roll	rad./sec.
q	Rate of Pitch	rad./sec.
r	Rate of Yaw	rad./sec.
t	Time	sec.
α	Angle of Attack	rad.
β	Angle of Sideslip	rad.
ψ	Angle of Yaw	rad.
ϕ	Angle of Roll	rad.
ϕ_o/ψ_o	Ratio of Roll to Yaw Angle at $t = o$	
θ	Phase Angle between Roll and Yaw oscillation	rad.
ω	Frequency of model oscillation	rad./sec.
λ	Wavelength of model oscillation = $\frac{2\pi V}{\omega}$	ft.

3.0 TEST METHODS

3.1 General

The problems concerning the aeroballistic range testing of aeroplane models will be discussed under the following headings: methods of construction, pre-flight measurements, launching, in-flight measurements and analysis of results. The first four of these will be considered in turn in the following sections, and the analysis methods will be discussed later.

Figures 1 to 4 show some of the aeroplane models that have been tested in the range. The NRC Delta is an aspect ratio 2 model with an NACA 0003-63 aerofoil section and a 5 inch span. This configuration is currently being tested in the wind-tunnel of the High Speed Aerodynamics Laboratory of the National Aeronautical Establishment at Ottawa for damping in roll and damping in pitch, using a free oscillation half model technique. As static lateral and longitudinal stability derivatives are also being measured in the wind-tunnel, the model has been chosen as a means of "calibrating" the range technique to determine the accuracy of the results, and for general development of methods of manufacture, measurement and analysis. The Bell X-1 model, with a 5.6 inch span, is 1/60th full scale. The model shown, which was for a preliminary test, was made without some of the fuselage detail to simplify manufacture. The Avro CF-105 models are 1/120th scale, with wing spans of 5 inches and have been made in aluminum, brass and steel.

3.2 Methods of Construction

Of the models tested, the most complicated to produce has been

3.2 Methods of Construction (cont'd.)

the CF-105 and so a description of the methods used in its manufacture will embrace most of the problems that have arisen.

An important factor in the feasibility of aeroballistics range tests with such models is the accuracy and cheapness of their construction. In general, the surface finish and accuracy of profile should be up to the standard of high speed wind-tunnel models. With no method of recovering the models, however, a large number of them may be required, depending on the scope of the test program, and so a low cost per model is very desirable.

The method used at CARDE is a good compromise between these conflicting requirements. Master copies are first made of both top and bottom surfaces of the model as shown in Fig. 5, with suitable reference surfaces to establish the height and position of the fuselage datum. These masters are copied from a wind-tunnel model using a Deckel Pantograph Die-Sinker, (a contour milling machine) and are 1 1/2 times the model scale. The contours from the two masters are then transferred on to the top and bottom surfaces of a prepared blank, again using the Die-Sinker, to form the model. This blank is made up of two pieces joined by a 10-24 stud so that after the external form has been machined, the nose portion of the model can be removed as shown in Fig. 6 to facilitate the machining of the engine ducts and to enable ballast materials to be inserted in the nose. The external shape is completed by inserting and gluing in place the

3.2 Methods of Construction, (Cont'd...)

tab carrying the vertical fin and rudder and hand polishing all external surfaces.

The accuracy of profile attainable with this method is of the order of ± 0.002" and the finished models can be produced at a rate of less than 100 man-hours each, once the master and templates have been made. Thus if the aeroballistics program is considered as supplementary to a wind-tunnel program, the additional cost for a reasonable number of ten models would be about $6000 for models plus about $2000 for the preparation of the master. By way of comparison, the typical cost of a wind-tunnel model of similar scale is about $50,000 while for a large free-flight model, with full telemetry, the cost could be double this figure. Models of the latter type would, of course, be able to supply a wider variety of information than can presently be obtained from the simple CARDE models. As a means of reducing the cost and manufacture time further, alternative methods of investment casting, using the "lost wax" process, were also investigated, but found unsatisfactory because of the low strength of the casting material.

The elevator control deflection, as shown in Fig. 4, is machined integrally with the rest of the wing at an angle which will trim the aircraft to fly at a small lift coefficient during its flight. One convenience of the copying method of manufacture is that for such features as the elevators, whose deflection may differ from one round to the next, changeable inserts can be used in the master with no increase in the time for manufacture. This would also simplify the incorporation of a series of changes to study drag effects.

3.2 Methods of Construction, (Cont'd...)

Typical ballast arrangements are shown in Fig. 6 and will be discussed later. To locate the models in the sawdust butt for inspection after firing, a 2 millicurie source of Cobalt 60 was used. Although not large enough to cause handling difficulties, it provides sufficient radiation to enable the model to be located at a range of 25 feet using a directional Geiger counter on the 0.2 millirankine/meter/hour scale. Some comments concerning strength of construction will be made in Section 3.4 in connection with sabot design.

3.3 Pre-flight Measurements

Because the models are used only once, it is important not only that they should be manufactured accurately, but that the geometry and inertia characteristics of each model should be recorded before it is flown. The problem is more difficult with model aircraft than with missiles however because their shapes are more complicated, and new techniques of metrology had to be devised following a study of the methods in use at the NAE, RAE and NACA.

Under this heading, there are three types of measurements, those of the model's planform and profile dimensions, of the centre of gravity location and of the moments and product of inertia.

Planform dimensions, together with certain height measurements of the wing-tips, nose, etc., are required for determination of wing area, mean aerodynamic chord length and position and for use in yaw card reduction. To obtain these dimensions, the model is supported by an angle plate in various attitudes with a height gauge used to take the measurements.

3.3 Pre-flight Measurements, (Cont'd...)

Profile measurements for example on wing chord sections, require a more involved arrangement because of

(a) the need for establishing the spanwise and longitudinal position of the chord being measured and

(b) the need for a large number of points to be measured in order to define the profile.

In the case of the CF-105 models, these profiles were checked with templates using the template jig shown in Fig. 7. With this jig, the templates for several wing lower surface profiles and fuselage sections are held in their proper relative position, so that when the model is put in place, all sections can be checked simultaneously. Mating upper surface templates are used to check the upper surface profiles and any of the templates can be removed for carrying out independent checks during manufacture.

A second method, which is being used on the CF-105 and the NRC Delta models, is to locate a number of points along each of several chord positions by using a marking template which consists of a pre-drilled plate that fits over the wing and allows marks to be made at exact locations on the wing upper surface. The height of these upper surface points relative to the fuselage datum and the thickness through the wing can be compared with the corresponding values from drawings or geometry reports and the accuracy of the profile thereby determined. As noted earlier, the error of the wing profiles, as measured in this way, is about $\pm$ 0.002", on a mean aerodynamic chord of about 3".

The methods for measuring centre of gravity positions and the

3.3 Pre-flight Measurements, (Cont'd...)

moments and product of inertia have been described in Ref. 9 and will therefore not be mentioned here. Moments of inertia are accurate to $\pm$ 0.3% and ε, the inclination of the principal longitudinal axis below the fuselage datum, can be measured to $\pm$ 0.2°.

3.4 Launching

The method used to launch models of this type into the aeroballistics range is to support the model in a sabot carrier which is a snug fit in the diameter of the 5.9" smooth-bore gun. When the charge is ignited, the sabot is propelled down the barrel as a free piston under the action of the gas pressure and by the time the muzzle is reached, it has imparted to the model a speed slightly in excess of the test Mach number. On emerging from the barrel, the sabot breaks apart into four "petals" which must diverge sufficiently from the line of fire to be caught in the sabot trap at the entrance to the range (30 feet from the muzzle) allowing only the model to fly through the central 12 inch escape hole and on into the range. The requirements of the sabot are thus

(a) to accurately locate the model in pitch and/or yaw with respect to the barrel axis,

(b) to accelerate the model to test Mach number without damaging it, and

(c) to separate cleanly from the model outside the barrel so that the model is not unduly disturbed before entering the range.

Considering each of these in turn, first the location of the model in the sabot is shown in Figure 8a. The forward end of the fuselage

3.4 Launching, (Cont'd...)

is held by four red fibre supports profiled to suit the local fuselage section. Each of these pieces is carried by a web attached to one of the four quarters or petals into which the main sabot shell is divided. The "duck's tail" projection shown at the base of the model in Figure 4 fits into a mating recess in a cylindrical thrust pad on the bottom of the sabot. This pad is also divided into four quarters, each of which is screwed to one of the sabot petals. To change the incidence of the model in the sabot, the mating recess can be positioned higher or lower relative to the thrust pad and the profile of the fibre inserts at the front can be altered so that a total adjustment of $\pm$ 3.5° can be obtained without difficulty.

The design of the base of the model fuselage and of the sabot thrust pad to withstand the high acceleration loads in the gun required some development. Piezo pressure measurements are taken in the barrel so that the accelerations are known: for a muzzle velocity of 1800 ft./sec. the acceleration will reach a peak value of about 6000 g's. Past experience has shown that even though this high acceleration has a duration of only about $\frac{1}{4}$ millisecond, it is a safe design practice to choose the model and thrust pad material such that the maximum bearing pressure between the model and thrust pad (i.e., $\frac{\text{model wt. x peak g's}}{\text{normal contact area}}$) does not exceed their compressive yield strength.

Figure 8b shows a typical separation of the sabot from the model. These photographs were taken during a test of the CF-105 at BRL, using the smear technique with a 35 mm. Fastax camera. Because the four quarters of the sabot are held together by nothing more than thin tabs of metal at the four outer base positions, as soon as the interior of the sabot is subjected to the full ram pressure of the air outside the

3.4 Launching, (Cont'd...)

muzzle, the quarters open up much like the petals of a flower. First the fibre inserts lift off the forward fuselage, and then the quarters of the thrust pad pivot laterally and at the same time give the model a final forward kick before the separated petals fly laterally from the line of fire. It is because of this final push just as the sabot is separating that it is important to design the sabot so that it breaks apart symmetrically and does not jar the model laterally.

3.5 In-flight Measurements

The general arrangement of the range is shown in the model pictured in Fig. 9. The sabot and model are fired from the gun emplacement at the upper right, and after the model passes the sabot trap, it first travels through an entrance room where micro-flash photographs of it can be taken, and then into the range proper where schlieren or shadowgraph pictures are taken, and model trajectory and attitude angles are measured at each of the 80 yaw card positions down the range.

Velocity measurements are made by a system of light screens (not shown in Fig. 9) accurately surveyed in at 50 ft. intervals and connected to chronographs which measure the time of travel between successive light screens to the nearest microsecond. The error of this method is approximately 0.3 ft./sec. in 1500 ft./sec. Model retardation values, which are obtained by differencing successive velocity readings are therefore subject to an error of about 2 per cent with aluminum models.

Four schlieren stations are currently used, three with 16" mirrors, and one with 36" mirrors. In Fig. 10 typical schlieren

3.5 In-flight Measurements, (Cont'd...)

and shadowgraph pictures are shown for the Bell X-1, and the NRC-Delta models. The amount of detail of shock wave and flow behaviour is equivalent to that obtainable with a wind-tunnel schlieren system, but with the advantage of showing the complete pattern, with no interference from walls or stings.

Yaw cards are normally spaced at 5' or 10' intervals, although $2\frac{1}{2}$' intervals are used for models with a high frequency of oscillation, and are of increasing area with distance from the gun up to a maximum of 9' x 11'6". A system of tubular steel frames which carry a reserve roll of paper are used to hold the paper taut at the exact longitudinal location. By means of spring-loaded pins, reference marks for the horizontal and vertical datum lines can be made in the paper quickly and accurately.

A typical cut made in the yaw card paper by the Bell X-1 model is shown in Fig. 11. Angle of attack α is determined by measuring the amount by which the distance between the nose point and the horizontal tailplane cut differs from the value for $\alpha = 0$. Sideslip angle β can be found by measuring the displacement of the fin cut to one side or other of the nose point. Roll angle ϕ is measured directly between the wing line and one of the reference lines. The error in the measurement of attitude angles is from 0.05° to 0.1°, depending on the model configuration.

For flights where large angles of attack or yaw occur, this method for measuring α and β may be unsatisfactory if the cuts in the yaw card are poorly defined or if some of the reference points on the model are obscured. An alternative method which has been devised to cover such cases is the use of the "Flight Attitude

3.5 In-flight Measurements, (Cont'd...)

Shadowgraph" shown in Fig. 12. A model is mounted in a gimbal system so that it can be positioned in any combination of pitch, roll and yaw angles and these angles read directly from the protractors shown. Using a collimated light beam, a shadow of the model is cast on a screen and by orienting the model until its shadow fits the yaw card cut, the attitude angles of the model in flight are determined. The error in measurement with this apparatus is about $\pm$ 0.5°.

Lateral motion of the centre of gravity, i.e. the trajectory of the model, is measured between the model cut and the horizontal and vertical reference lines, and can be determined to within 1/16th of an inch.

The effect of yaw cards on the oscillations of the models is negligible for the small angle of attack range covered in most of the CARDE aeroplane experiments. This is evidenced by comparative tests in which identical missiles are fired first through closely spaced yaw cards and then through cards spaced at wide intervals. For angles of attack above about 10° there is some card interference effect on C_{M_α}, and a test program is currently under way to enable a quantitative correction to be made for this.

The effect of the yaw cards on the retardation of the model will be discussed in Section 5.3.

4.0 TEST RESULTS

Using the methods described in the preceding section, histories of α, β, Φ, Y_{CG} and Z_{CG} are obtained as shown in Figures 13a, b and c for three typical rounds. These three records are all for

4.0 TEST RESULTS, (Cont'd...)

the same configuration, at nominally the same Mach number, and a comparison of them shows the effect of CG position and inclination of the principal longitudinal axis of inertia. The round of Fig.13a has a forward CG position at 8.7% MAC and the record will be seen to consist of a small, rapidly-damped oscillation in pitch, while in yaw and roll there is a coupled Dutch roll oscillation of lower frequency but much larger amplitude. The points occur at the yaw card positions with intervals of 5' or 10' and at a sufficient frequency to give a good record of the shape of the β or ϕ curve. In Fig. 13b the CG is at 19.2% MAC and the frequency of roll, pitch and yaw have all decreased while the damping has changed from being positive to slightly negative.

For these two rounds, the principal axis of inertia was inclined at about 2° below the fuselage datum. For the model of Fig.13c, the CG is still further aft, at 22.9% MAC, but by ballasting with inserts as described earlier, the principal axis inclination ϵ has been reduced from 2° to 0 and the strong effect of this is obvious. The Dutch roll is of much smaller amplitude than before, and is heavily damped. The oscillation in pitch, on the other hand, is of larger magnitude than for the previous rounds and shows no signs of cross-coupling from the roll or yaw, i.e. there is no modulation of the motion at the roll frequency. In this case, an initial displacement in pitch was achieved by mounting the model in the sabot at a positive angle of attack.

The fact that by suitable ballasting and sabot design, either a pure pitching oscillation or a Dutch roll lateral oscillation with negligible cross-coupling can be selected is of considerable

4.0 TEST RESULTS, (Cont'd...)

importance in the analysis of the results. It means that simple one or two degree of freedom solutions, which are amenable to manual methods of calculation, can be used to extract the necessary stability derivatives. In terms of time, this means that firing models of a series at a rate of one per week, it is possible for two people to analyse the test results of one round before the next model is fired. This compares favourably with the amount of data reduction required for free flight tests using telemetry.

5.0 ANALYSIS

5.1 Lateral Stability Derivatives

Various methods of analysing this type of record have been considered. An analogue method of curve fitting has been applied to some of the test results[10] and has given derivative values in good agreement with those of other methods, although this approach does not appear well suited to solutions where three or more degrees of freedom are involved. Another method, which has been developed at Avro Aircraft for the analysis of their large scale ground-launched free-flight models and at the Cornell Aeronautical Laboratory is an extension of Doetsch's time vector method[11] to lateral as well as longitudinal motions.[12, 13, 14]

The method which will be described here was developed by Mr. R. J. Templin at NAE and has proved very useful for the analysis of the Dutch roll motion. Referring again to the records of α, β, and ϕ in Figures 13a, b and c, it has already been noted that the pitching motion is small enough that any roll-pitch cross-coupling can be neglected. The oscillation in roll is super-imposed on a slow steady

5.1 Lateral Stability Derivatives, (Cont'd...)

rate of roll while the yawing motion is at the same frequency, with a slight shift in phase and approximately the same rate of damping.

Considering the records of the lateral co-ordinates of the model centre of gravity Y_{CG} and Z_{CG}, there is no apparent ripple at the Dutch roll frequency. Thus it may be assumed that the angle of yaw ψ is equal to $-\beta$, the sideslip angle. The implication of this assumption is that aerodynamic side forces are negligible, and therefore that in the equations of motion, the side force equation can be neglected, leaving only the two equations for yawing and rolling moments.

Making use of the above assumptions, these equations are as follows:

$$\frac{d^2\phi}{dt^2} - \frac{I_{xz}}{I_x}\frac{d^2\psi}{dt^2} = \frac{1/2\ \rho\ V^2\ Sb}{I_x}\left\{C_{l_\beta}\ \beta + C_{l_p}\left(\frac{pb}{2V}\right) + C_{l_r}\left(\frac{rb}{2V}\right)\right\} \quad \ldots(1)$$

$$\frac{d^2\psi}{dt^2} - \frac{I_{xz}}{I_x}\frac{d^2\phi}{dt^2} = \frac{1/2\ \rho\ V^2\ Sb}{I_z}\left\{C_{n_\beta}\ \beta + C_{n_p}\left(\frac{pb}{2V}\right) + C_{n_r}\left(\frac{rb}{2V}\right)\right\} \quad \ldots(2)$$

where $\beta = -\psi$, $r = \dot{\psi}$ and $p = \dot{\phi}$

On the basis of the character of the records, (and considering only the oscillatory part of the ϕ record) a solution of the form shown below is assumed:

$$\psi = \psi_o\ e^{-kt}\ \sin \omega t \quad \ldots(3)$$

$$\phi = \phi_o\ e^{-kt}\ \sin (\omega t + \theta) \quad \ldots(4)$$

5.1 Lateral Stability Derivatives, (Cont'd...)

ωt is set equal to zero and alternatively to $\pi/2$ in equations (3) and (4) and in the corresponding equations for the first and second derivatives of ψ and ϕ. The two sets of values thus obtained are substituted into equations (1) and (2), resulting in the following four algebraic equations:

$$A_1 + \frac{2I_{xz}}{I_x} k\omega - R_1 C_{l_r} + P_1 C_{l_p} = 0 \qquad .....(5)$$

$$A_2 + 2k\omega + R_2 C_{n_r} - P_2 C_{n_p} = 0 \qquad .....(6)$$

$$A_3 + \frac{I_{xz}}{I_x} (\omega^2 - k^2) + R_3 C_{l_r} + P_3 C_{l_p} + \frac{qSb}{I_x} C_{l_\beta} = 0 \qquad ...(7)$$

$$-A_4 - (\omega^2 - k^2) + R_4 C_{n_r} + P_4 C_{n_p} + \frac{qSb}{I_z} C_{n_\beta} = 0 \qquad ....(8)$$

where

$$\left.\begin{aligned}
A_1 &= -\frac{\phi_o}{\psi_o}\left[(\omega^2 - k^2) \sin\theta + 2k\omega \cos\theta)\right] \\
A_2 &= \frac{I_{xz}}{I_z} A_1 \\
A_3 &= \phi_o/\psi_o\left[-(\omega^2 - k^2) \sin\theta + 2k\omega \sin\theta)\right] \\
A_4 &= \frac{I_{xz} A_3}{I_z} \\
R_1 &= \frac{\rho V S b^2 \omega}{4 I_x} \\
R_2 &= \frac{I_x}{I_z} R_1 \\
R_3 &= \frac{\rho V S b^2 k}{4 I_x} \\
R_4 &= \frac{I_x R_3}{I_z}
\end{aligned}\right\} \qquad ....(9)$$

5.1 Lateral Stability Derivatives, (Cont'd...)

$$P_1 = \frac{\rho VSb^2}{4I_x} \frac{\phi_o}{\psi_o} (k \sin \theta - \omega \cos \theta)$$

$$P_2 = \frac{I_x}{I_z} P_1$$

$$P_3 = \frac{\rho VSb^2}{4I_x} \frac{\phi_o}{\psi_o} (k \cos \theta + \omega \sin \theta)$$

$$P_4 = \frac{I_x}{I_z} P_3$$

When appropriate values of amplitude ratio ϕ_o/ψ_o, frequency ω, damping factor k and phase angle θ are substituted into equations (5) to (8), the only remaining unknowns are the six lateral stability derivatives C_{l_β}, C_{n_β}, C_{l_p}, C_{n_p}, C_{l_r} and C_{n_r}. With six unknowns in a set of four simultaneous equations, two of the derivatives must be assumed in order to solve for the remaining four. It was considered preferable to solve for C_{l_β}, C_{n_β}, C_{l_p}, as these three could most easily be verified from previous tests, and of the remaining three, it was decided to assume C_{l_r} and C_{n_r} because of the small size of the terms in which they occur.

Most of the test results so far obtained using this method have been for the CF-105 aircraft and although quantitative results are still classified, a bar graph comparison is given in Figure 14 of the derivative values from the NACA Langley and Cornell wind tunnel tests, the 1/8th scale free flight tests, and the CARDE test results.

5.1 Lateral Stability Derivatives (Cont'd.)

The CARDE values of C_{l_β}, C_{n_β} and C_{l_p} lie close to those obtained from the wind-tunnel tests and those obtained in 1/8th scale free flight tests at Avro. C_{n_p} agreement was not so good, although the check here was against an estimated value. Typical comparisons of lateral derivative values from the analysis of the Bell X-1 and NRC Delta model records are given in Table I and in Fig. 15a. The NAE wind tunnel valves of C_{n_β} and C_{l_β} are in good agreement with the CARDE test curves.

In using this type of analysis for a test program in conjunction with preliminary wind-tunnel tests, it would probably be more advisable to use the wind-tunnel values of C_{n_β} and C_{l_β} as the assumed values in the equations, and solve for the four rotary derivatives, as these are more difficult to evaluate in the wind-tunnel.

5.2 Longitudinal Stability Derivatives

Analysis of the pitching oscillation to determine longitudinal stability derivatives is somewhat simpler than for the lateral case. Measurements of the frequency of the oscillation ω and the damping rate k are made and C_{M_α} can be found directly from the relation:

$$C_{M_\alpha} = \frac{-2I_Y\omega^2}{\rho V^2 S\bar{c}} = \frac{-2I_Y}{\rho S\bar{c}} \left(\frac{2\pi}{\lambda}\right)^2 \qquad \ldots\ldots\ldots\ldots \quad (10)$$

5.2 Longitudinal Stability Derivatives (cont'd.)

A cross-plot of C_{M_α} vs. CG position for several rounds at the same Mach number will give C_{L_α} as its slope and the aerocentre position as the intercept value of CG position for which $C_{M_\alpha} = 0$.

The damping in pitch $(C_{M_{\dot{\alpha}}} + C_{M_q})$ is then obtained from the equation below:

$$C_{M_{\dot{\alpha}}} + C_{M_q} = \frac{2 g I_Y}{W\overline{c}^2} C_{L_\alpha} - \frac{8 I_Y k}{\rho V S \overline{c}^2} \quad \ldots\ldots\ldots\ldots \quad (11)$$

Some of the values so obtained for the Bell X-1, Avro CF-105 and the NRC Delta are shown in Table I, Fig. 14 and Fig. 15b. The good agreement of both C_{M_α} and $(C_{M_{\dot{\alpha}}} + C_{M_q})$ with wind-tunnel values will be noted.

5.3 Drag

One of the most important applications of the free flight technique is the measurement of aeroplane drag. The aeroballistics range method has the advantage over the ground-to-air technique that the air in the range is at rest and is of constant density so that wind and altitude corrections are not necessary. There is also no correction for the effect of the gravity component on longitudinal acceleration because the trajectory is very nearly horizontal. Furthermore, the data reduction with the light screen system used to measure velocity is very simple in comparison with that required for the Doppler radar apparatus. Another distinct advantage is that the models are so cheap to produce that a whole series of tests

5.3 Drag (cont'd.)

making small configuration changes to determine their effect on drag can be completed for the cost of one or two large fully-telemetered rounds.

As described in Section 3.5, the time of flight between accurately located light screens is measured using Potter chronographs to determine the velocity at 50 ft. intervals down the range. The difference between these successive velocities or the retardation bears the following relation to the model's drag coefficient.

$$C_D = \frac{W}{g} \times \frac{aM}{50} \times R_{50} \times \frac{1}{0.7\ pM^2\ S}$$

$$= \frac{W\ a\ R_{50}}{1127\ pMS} \qquad \text{..... (12)}$$

where R_{50} is the retardation in feet per second per 50 ft.

As mentioned earlier, the error of the measuring equipment is of the order of 2 percent on drag. One difficulty with the use of yaw cards however is that part of this measured retardation is due to the effect of the yaw cards. Comparison of CARDE test results with those obtained using the same configuration (CF-105) at BRL, where only photographic methods of measurement are used, indicates an effect which is of the order of 4%. Although it might be possible to use a correction factor to compensate for this, the current plans will enable drag to be measured down-range of all the yaw cards to completely eliminate this error. Drag values obtained for the

5.3 Drag (cont'd.)

current models are listed in Table I and Fig. 15b. The comparison with the drag of the Bell X-1A is quite good.

6.0 FUTURE PLANS

The plans for further development of aeroplane testing in the aeroballistics range are closely related to the limitations of the present methods, and so the two can be discussed together.

Concerning manufacture and inspection methods, the two limitations of the present models are the extent of simulation of detail, because of the physical size of the models, and the limit in launch speed, because of structural difficulties. Under consideration at CARDE is a 14" gun which would permit double the scale of present models and simplify the manufacture and inspection problems. As launch speeds are increased, the inertia load of the model on its thrust pad increases rapidly so that for practical purposes the models described here would be limited to a Mach number of about 3. In the design stage at CARDE is a light gas gun which will permit this limit to be raised to Mach 10 for models of the present size.

A weakness of the range instrumentation as described here is the lack of any direct method of measuring lateral accelerations of the model. With such information, direct determination of force derivatives C_{L_α} and C_{Y_β} would be possible and greater accuracy could be obtained in the determination of drag in the absence of yaw cards. Under development by a subcontractor is a very small telemetry set to meet this need which would fit inside the model

6.0 FUTURE PLANS (cont'd.)

and transmit on two or three channels.[15] Early trials of the set have been encouraging. In addition to the application above, such an instrument could be used for such purposes as surface temperature measurements or the determination of hinge moments.

In future work, it is hoped to determine control effectiveness C_{M_δ} by using a variety of elevator deflections on successive models and making use of the relation:

$$C_{M_\delta} = \frac{C_{M_\alpha}}{\alpha_T/\delta} \quad \text{where } \alpha_T \text{ is the steady state trim value}$$

of angle of attack. One drawback of the range in comparison with either wind tunnels or ground-launched free flight models is that there is a limited range of trimmed lift coefficients for which the model will stay within the region covered by the range instrumentation. This results in a limitation in the amount of elevator deflection which can be used for the C_{M_δ} determination above, and also means that the drag measurements have to be carried out very nearly at the zero-lift condition. This restriction can of course be relaxed to some extent by simply allowing the model to fly off to the side of the range before it has reached the end. As an example, if a steel delta model of 5" span flying at $M = 1.6$ could be allowed to diverge 6' laterally in the first 150 ft. from the gun, a lift coefficient of 0.14 could be attained.

One field where much additional work can be done in these studies is in the extension of methods of analysis of the records. Some

6.0 FUTURE PLANS (cont'd.)

time has been spent in applying the modified Fourier Transform method given in Ref. 16. The poor derivative values which resulted from the use of manual methods of integration indicate the need for a digital computer however, and a further study of the method is underway at present using the ALWAC III computer.

7.0 CONCLUSIONS

Tests carried out in the aeroballistics range using small scale delta and straight-winged aircraft models have established that:

(a) Manufacturing methods have been developed by which solid metal models can be manufactured at a rate of about 100 manhours each to an average profile tolerance of ± 0.002".

(b) Special care must be taken to check wing profiles and model contours prior to firing. Methods of measuring model moments and products of inertia have been developed.

(c) Models have been successfully launched into the range at speeds up to Mach 2.6 (Reynolds number about 4.7 million based on MAC) and with present equipment, launch speeds of Mach 3.0 should be attainable.

(d) During the model's free flight down the range, its roll, pitch and yaw angles can be measured to within 0.1 degrees and lateral centre of gravity position to the nearest sixteenth of an inch, using yaw card techniques. In addition, the model's velocity history can be determined, using a light screen system, to the nearest 0.3 ft/sec., while shock wave and flow visualization are obtained with schlieren

7.0 CONCLUSIONS (cont'd.)

(d) (cont'd.)
systems.

(e) With suitable ballasting of the model and positioning of the model in the sabot, either a Dutch roll type of motion or a longitudinal pitching motion can be obtained independently, thus enabling the use of much simplified methods of analysis to determine the lateral or longitudinal stability derivatives.

(f) With the simple methods of analysis currently in use, reasonably close agreement can be achieved to stability derivatives determined in wind-tunnels and with large scale ground-launched free flight models.

(g) The velocity-measuring system gives retardation values to an accuracy of 2%. A small drag increment due to yaw card interference has been noted (4%).

Although further development of the technique is needed to exploit all its possibilities, the results obtained so far have shown that the aeroballistics range can be a useful tool in determining the performance and lateral and longitudinal stability characteristics of high speed aircraft. The cheapness of the model construction and simplicity of data reduction make the method attractive in comparison to large-scale rocket-launched free flight models. However it shares with such techniques the advantage over wind-tunnels of giving high Reynold's number dynamic test data which are free from any possible errors due to tunnel wall or sting support corrections.

7.0 CONCLUSIONS (cont'd.)

It is therefore felt that the type of test reported on here could prove useful not only to supplement the standard wind tunnel program for a final design of aircraft, but could be used at an earlier stage in design, before the "lines" had been frozen, so that configurational changes specifically to improve the dynamic stability and drag characteristics could still be made.

REFERENCES

1. References to Range Facilities:

   (a) W. Rogers - The Transonic Free-Flight Range. APG/BRL Report 849.

   (b) Proceedings of the Aerodynamic Range Symposium Jan. 1957. APG/BRL Report 1005, Part I, March 1957.

2. G.V. BULL — Aeronautical Studies in the Aeroballistics Range. CARDE Report 302/57, July 1957.

3. G.H. TIDY & MISS M.E. THOMAS — An Application of Aeroballistics Range Techniques to Models with Digonal Rotational Symmetry. CARDE TM AB-21 (To be published)

4. A. SEIFF — A Free-Flight Wind Tunnel for Aerodynamic Tests at Hypersonic Speeds. NACA Report 1222 1955

5. D.D. BAALS — Model Selection and Design Practices Applicable to the Development of Specific Aircraft. AGARD Report 21 Feb. 1956.

6. J.A. SHORTAL — Techniques of Model Testing in Free Flight. Wind Tunnel & Model Testing Panel. AGARD May 3-7, 1954.

7. J.A. HAMILTON & P.A. HUFTON — Free Flight Techniques for High Speed Aerodynamic Research. Journal of the Royal Aeronautical Society. Vol. 60, No. 543, March 1956.

8. K. ORLIK-RUCKEMANN — Methods of Measurement of Aircraft Dynamic Stability Derivatives. NAE Quarterly Bulletin - Report No. NAE 1957(4) December 1957.

9. H.R. WARREN — Measurements of Model Aeroplane Moments & Products of Inertia. CARDE TM AB-31 Sept. 1957

10. D. TAIT & H.R. WARREN — REAC Analysis of Aeroballistics Range CF-105 Test Data. CARDE TM A5-51 June 1958.

11. K.D. DOETSCH — Time Vector Method for Stability Investigations. RAE Report Aero 2495 Aug. 1953.

12. M.V. JENKINS — Time Vector Analysis of Free Flight Model Lateral Results. Avro Aircraft Ltd. P/Stability/135 1957.

13. M.V. JENKINS — Time Vector Analysis of Free Flight Model Longitudinal Results. Avro Aircraft Ltd. P/Stability/140 1957

14. E.E. LARRABEE — Application of the Time Vector Method to the Analysis of Flight Test Lateral Oscillation Data. Cornell Aeronautical Laboratory FRM 189 Sept. 1953.

15. D.E. DUFF — Ballistics Range Telemetry System Speeds Data Recording. Canadian Electronic Engineering Dec.1957

16. M. SHINBROT — On the Analysis of Linear and Nonlinear Dynamical Systems for Transient Response Data. NACA TN 3288 December 1954.

17. H.S. RIBNER & F.S.MALVESTUTO — Stability Derivatives of Triangular Wings at Supersonic Speeds. NACA Report 908, 1948.

18. H.R. WARREN & F.B.SNELGROVE — Aeroballistics Range Tests of the Bell X-1 Aircraft. CARDE TM AB-24 June 1958.

ACKNOWLEDGMENTS

The author expresses appreciation of the cooperation and contributions to this work of Mr. R. J. Templin of the National Aeronautical Establishment and Mr. B. Cheers of CARDE.

TABLE I

COMPARISON OF AERODYNAMIC DATA FOR THE BELL X-1 AIRCRAFT
(Ref: 18)

(C.G. 22.3% M.A.C.)

Derivative	M	CARDE Value	NACA Value
C_{M_α} per deg.	1.2	-0.038	-0.03
C_{n_β} per deg.	1.2	.0069	0.004
C_{l_β} per deg.	1.2	-0.00275	-0.0018
C_{l_p} per rad.	1.2	-0.40	-0.41
C_{n_p} per rad.	1.2	0.313	----
C_{D_o}	1.2	0.14	0.144

FIGURE I
NRC DELTA MODEL

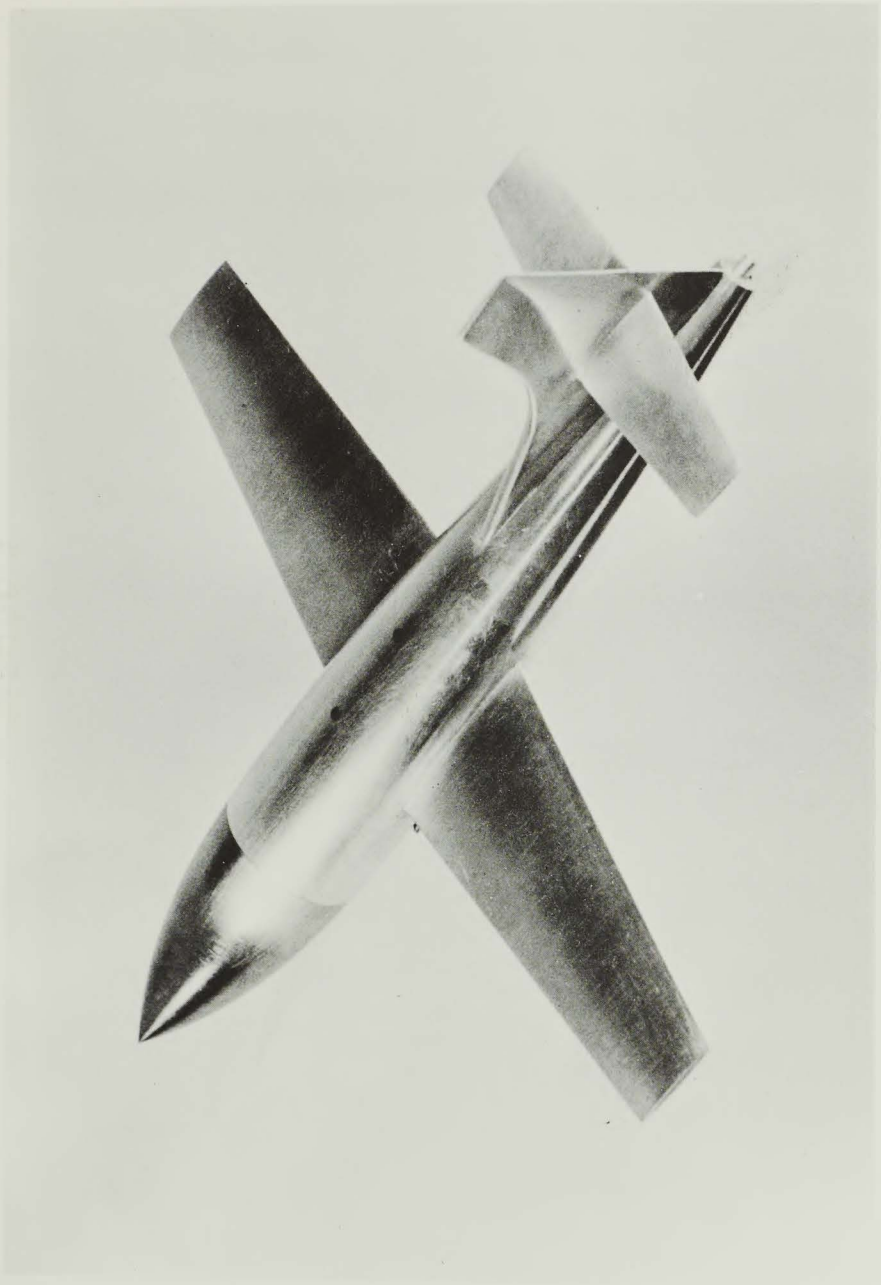

FIGURE 2
BELL X-1 MODEL

FIGURE 2
BELL X-1 MODEL

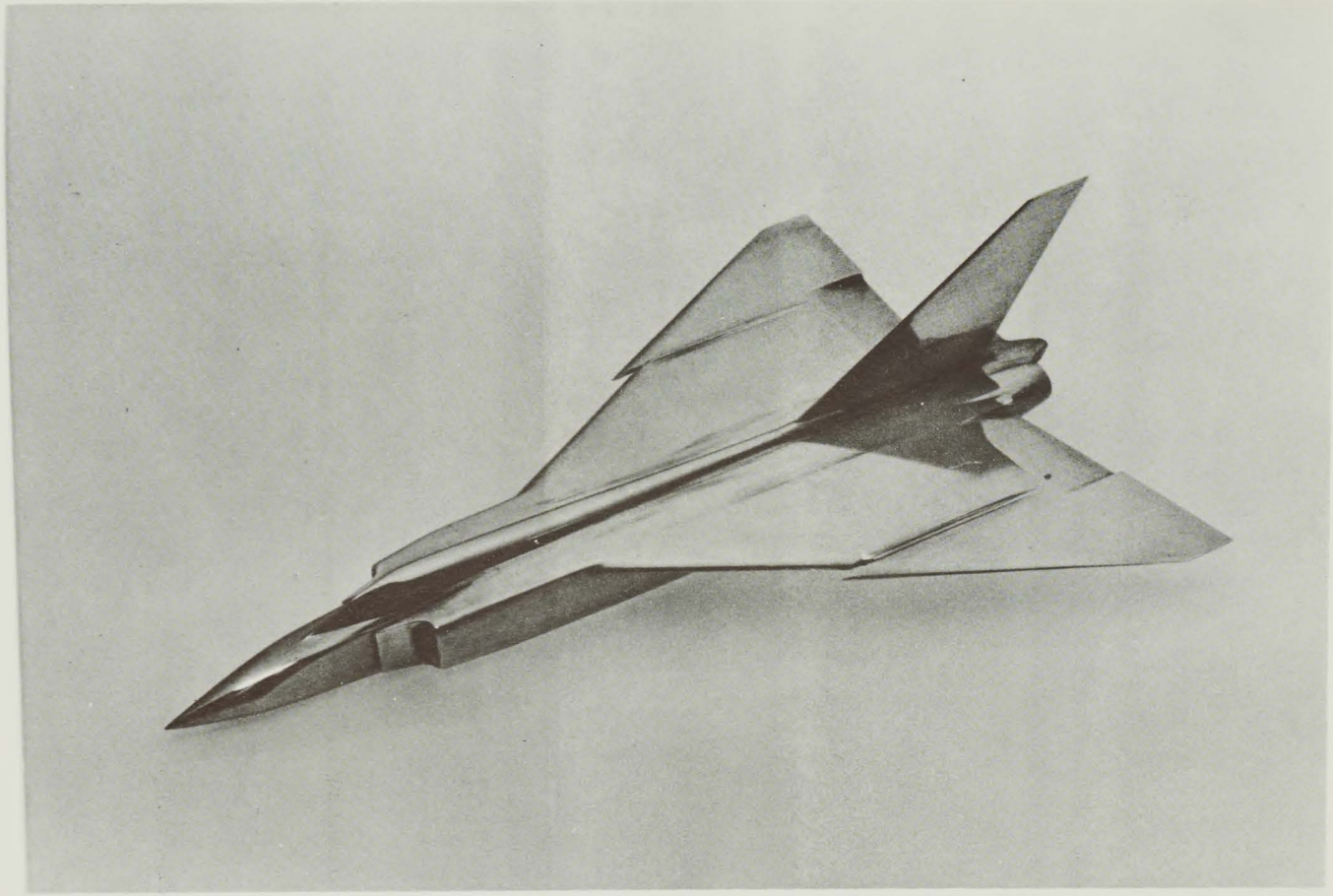

FIGURE 3
AVRO CF-105 MODEL FRONT VIEW

FIGURE 4
AVRO CF-105 MODEL REAR VIEW

FIGURE 5
CF-105 COPYING MASTERS

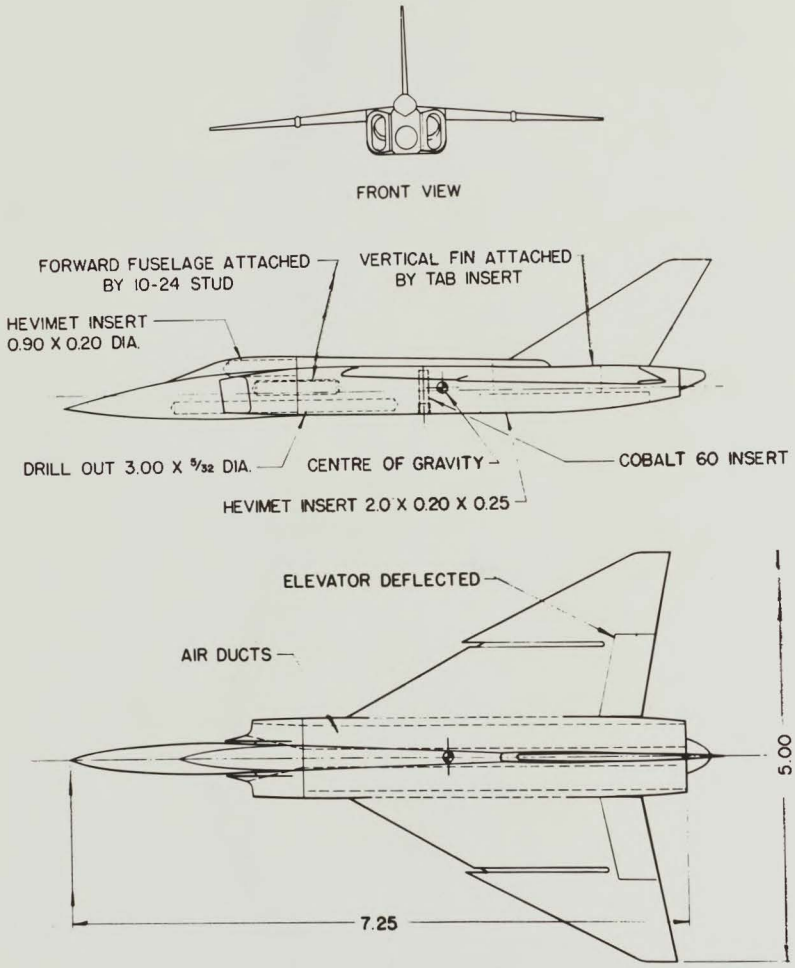

FIGURE 6
DETAILS OF CONSTRUCTION OF CF-105 MODEL

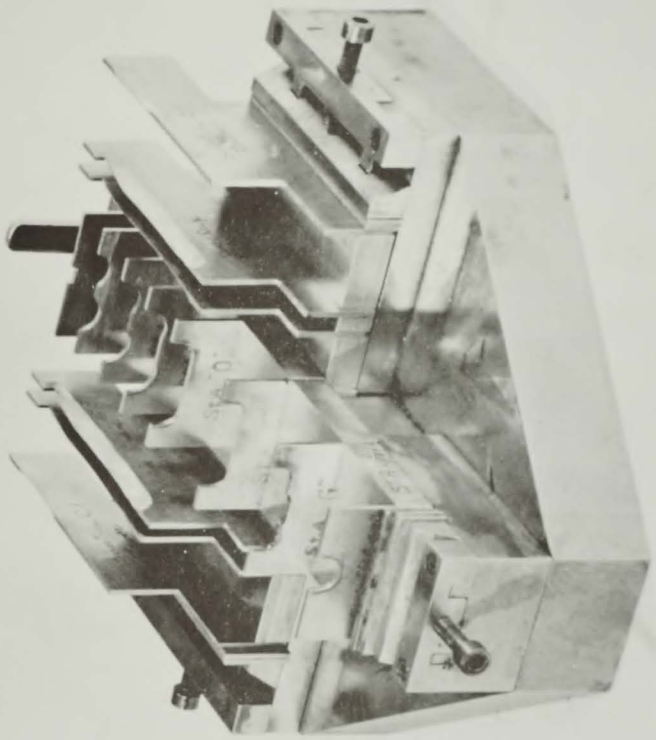

FIGURE 7
CF-105 TEMPLATE JIG

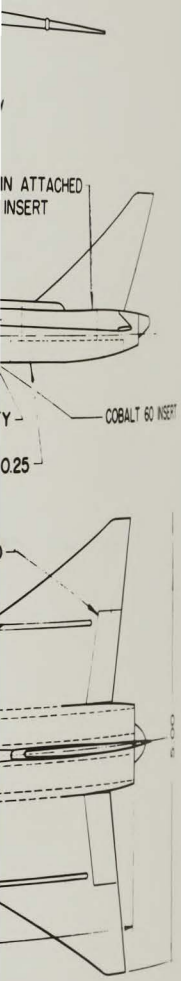

OF CF-105 MODEL

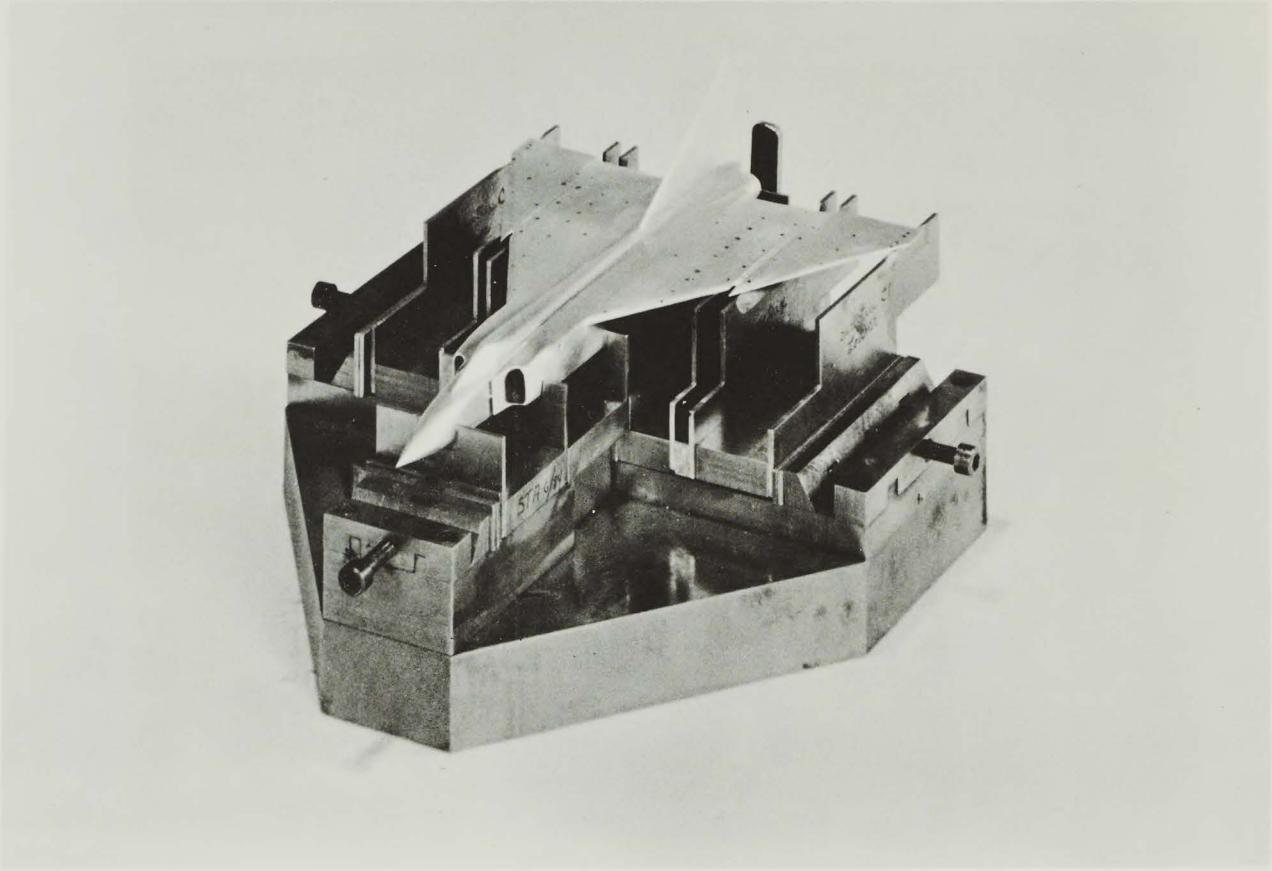

FIGURE 7a

CF-105 TEMPLATE JIG

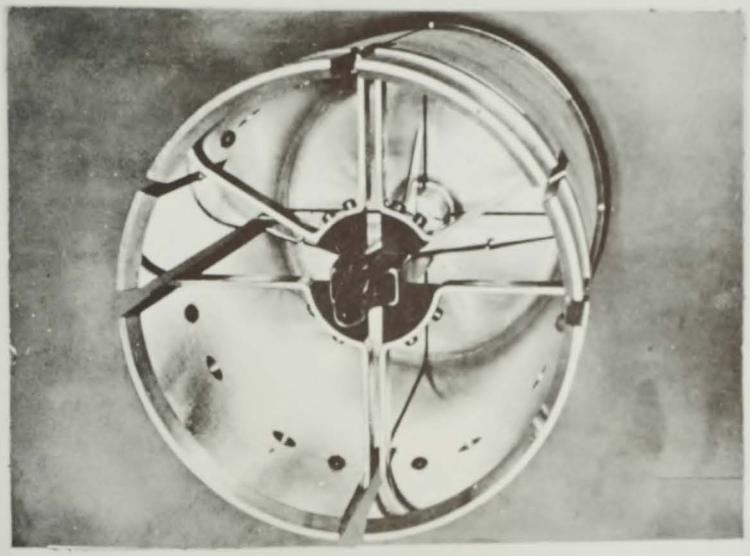

FIGURE 8a
CF-105 MODEL IN SABOT

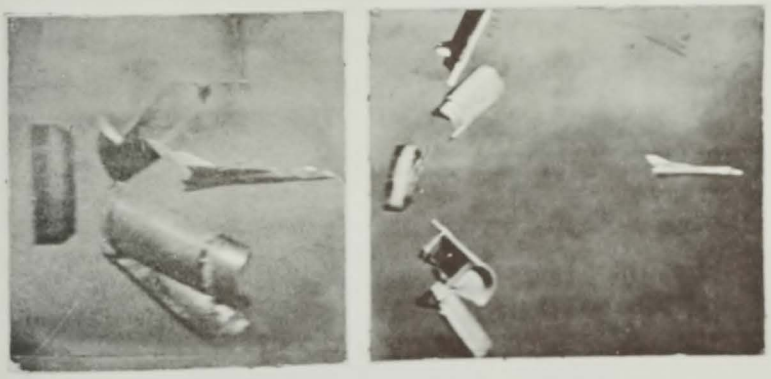

FIGURE 8b
SEPARATION OF SABOT FROM MODEL

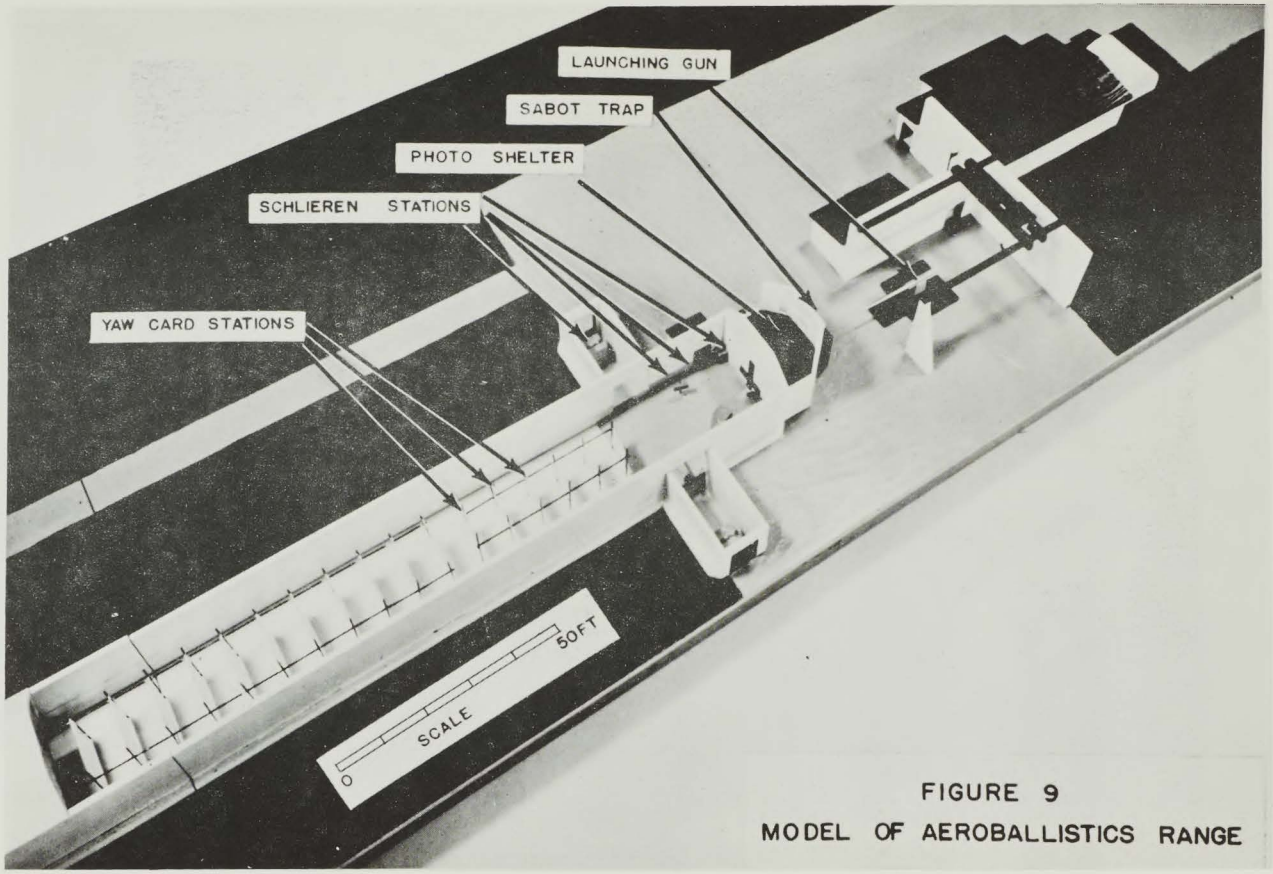

FIGURE 9
MODEL OF AEROBALLISTICS RANGE

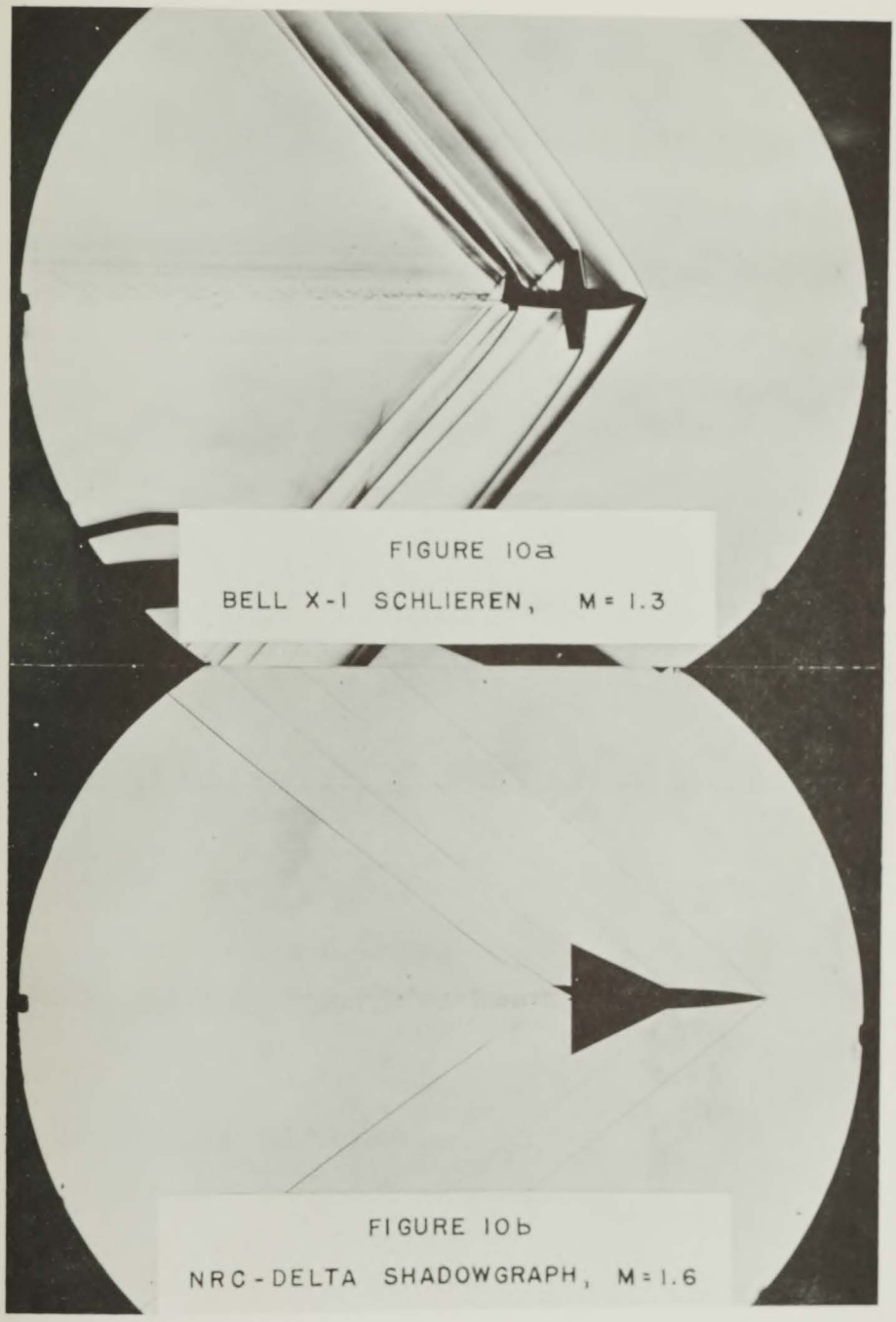

FIGURE 10a

BELL X-1 SCHLIEREN, M = 1.3

FIGURE 10b

NRC-DELTA SHADOWGRAPH, M = 1.6

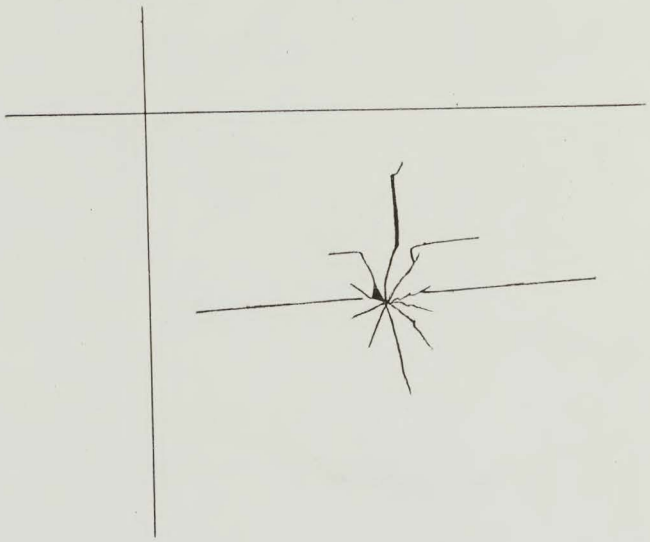

$M = 1.3$ $\alpha = +0.3°$

$\phi = -4.0°$ $\beta = +2.4°$

FIGURE 11

TYPICAL YAW CARD CUT

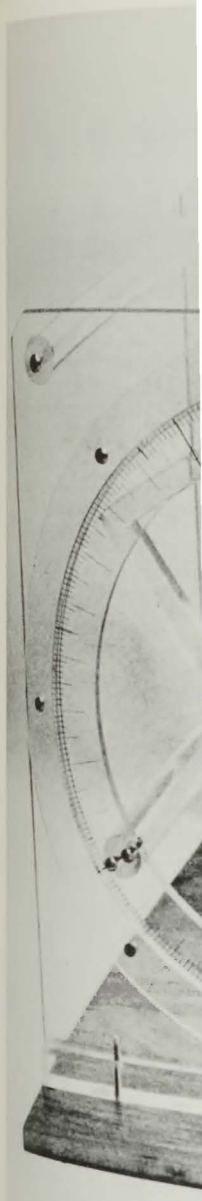

FLIGHT

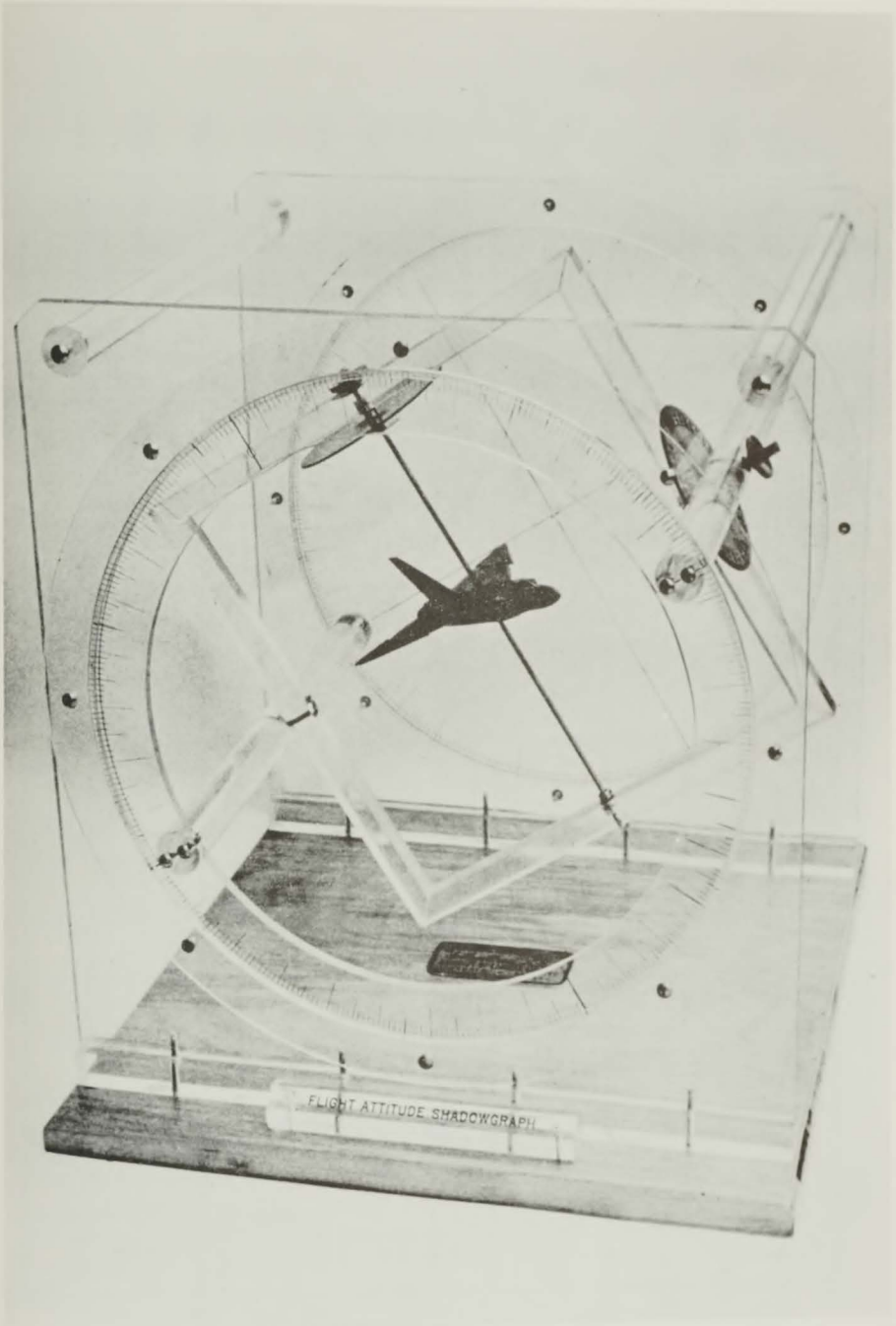

FIGURE 12
FLIGHT ATTITUDE SHADOWGRAPH

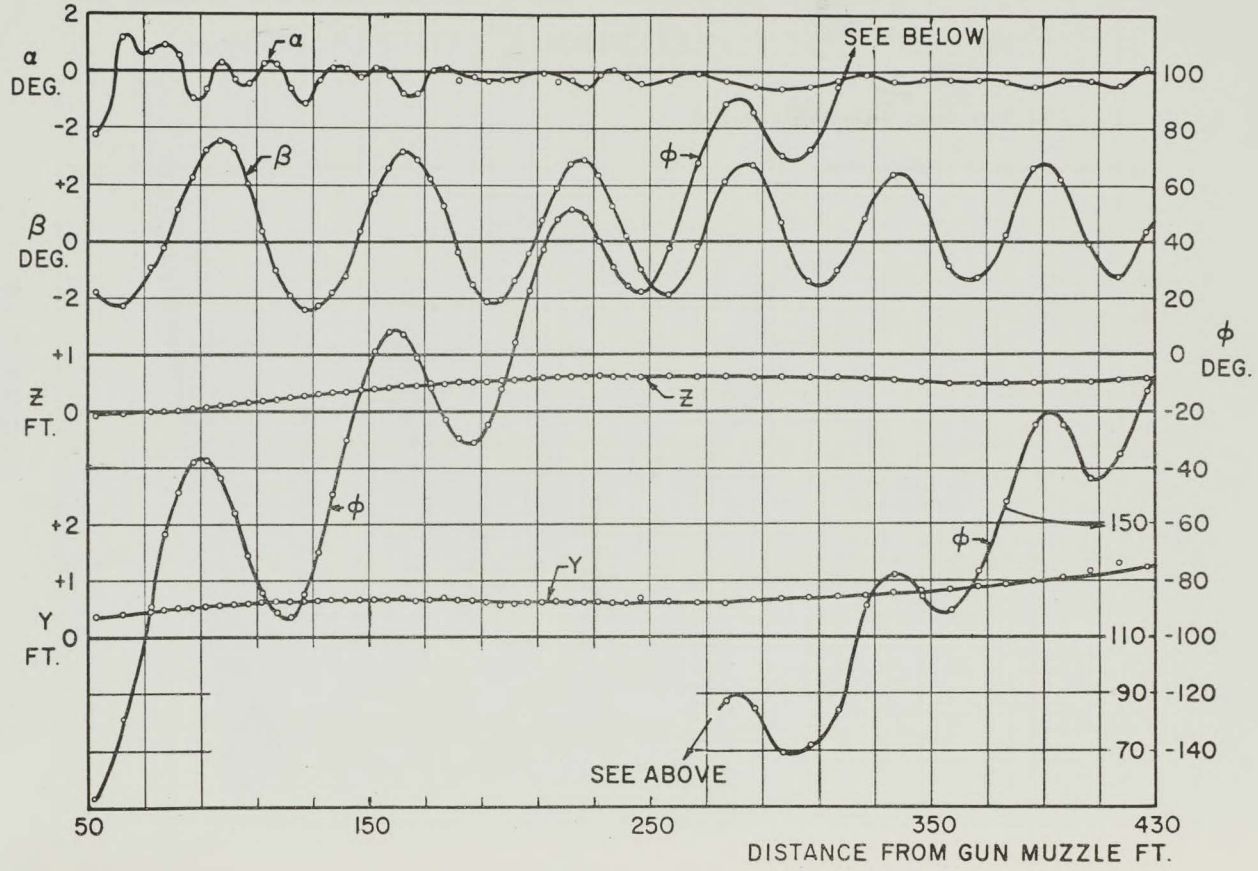

FIGURE 13a

TEST RECORD FOR FORWARD CG, (8.7 % MAC) $\varepsilon = 2^\circ$

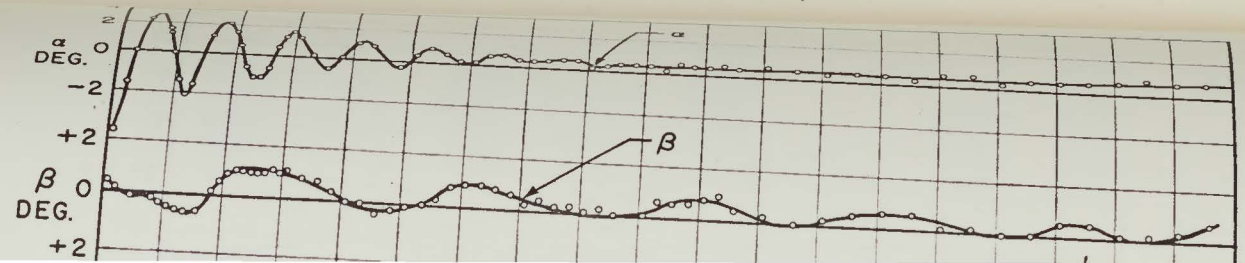

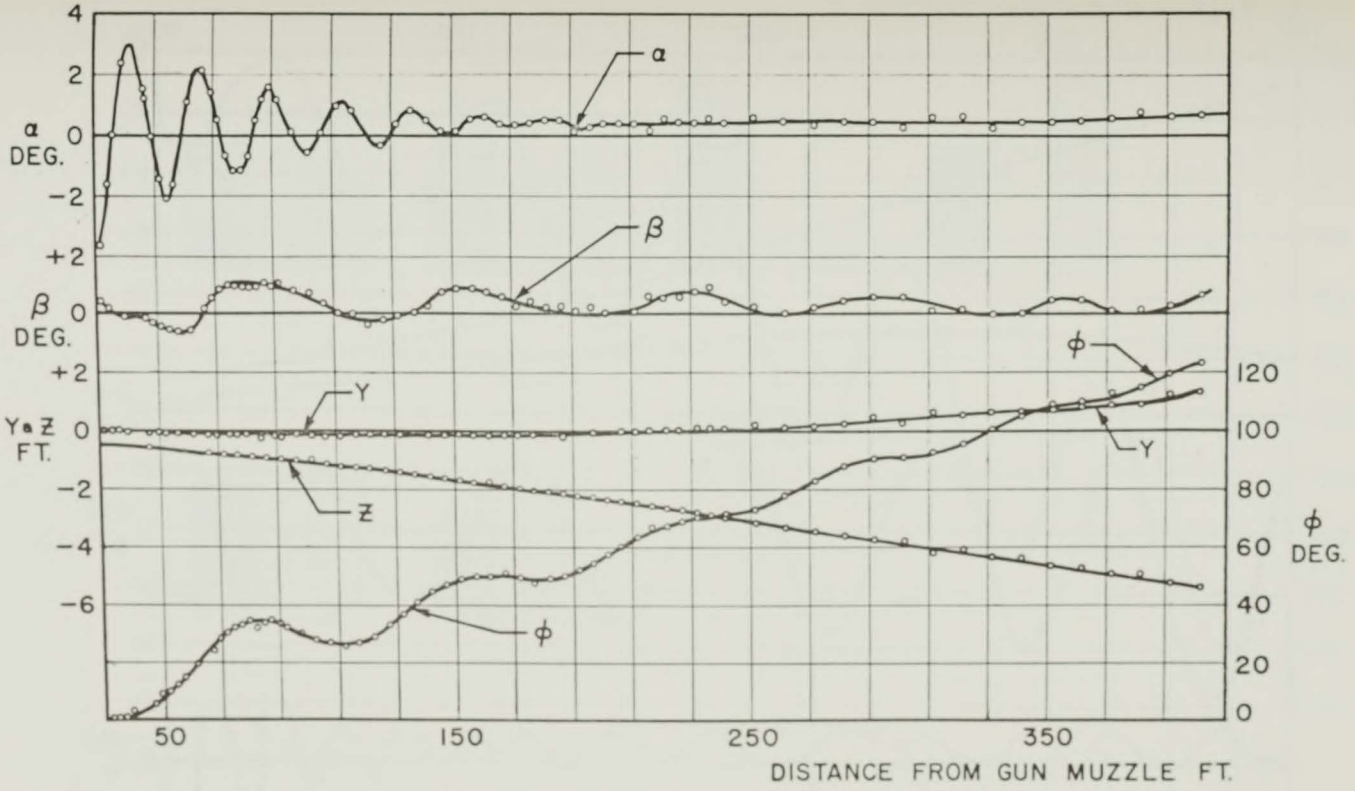

FIGURE 13c

TEST RECORD FOR AFT CG (22.9% MAC) $\varepsilon = 0^\circ$

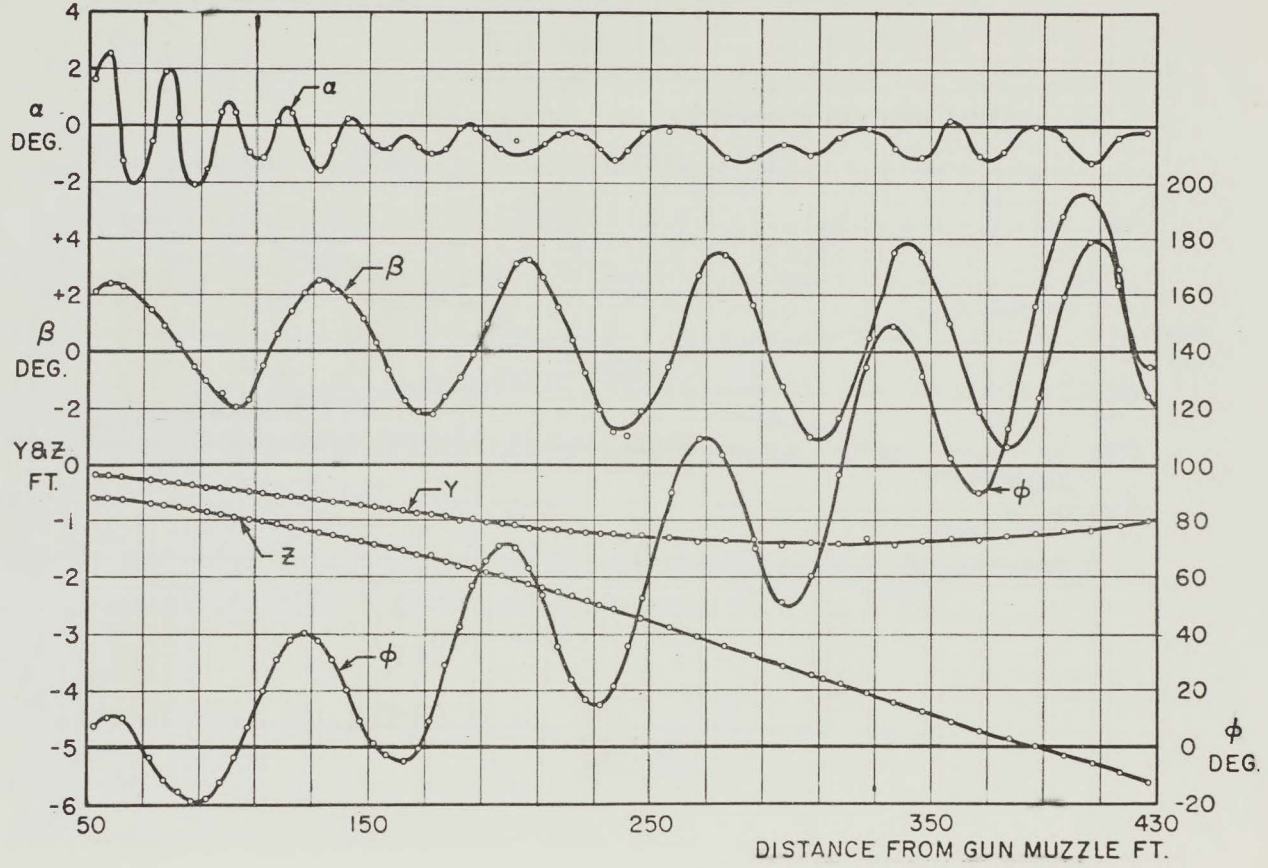

FIGURE 13b

TEST RECORD FOR AFT CG, (19.2% MAC) $\varepsilon = 2°$

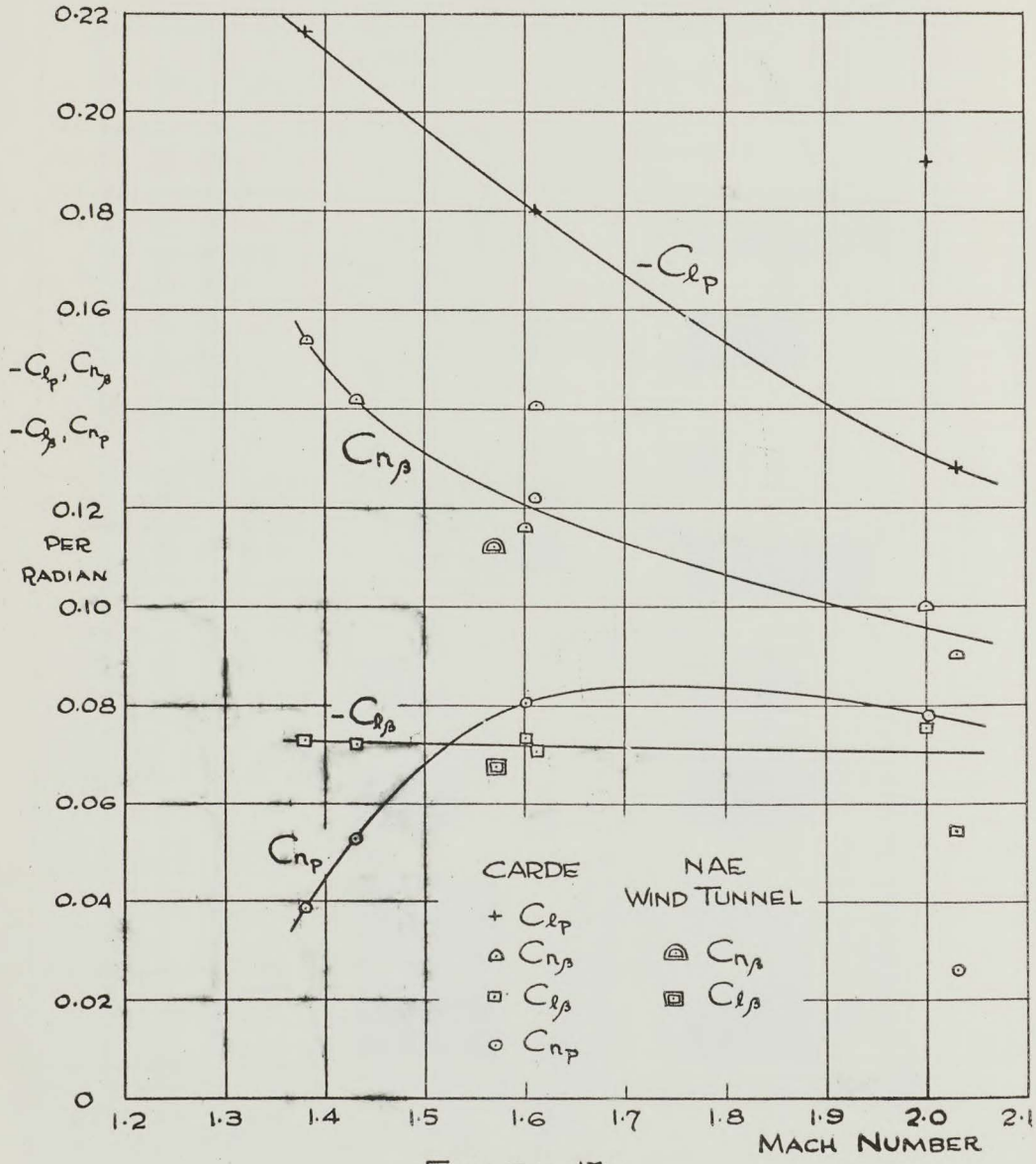

FIGURE 15a
NRC-DELTA LATERAL DERIVATIVES
(CG 13% MAC)

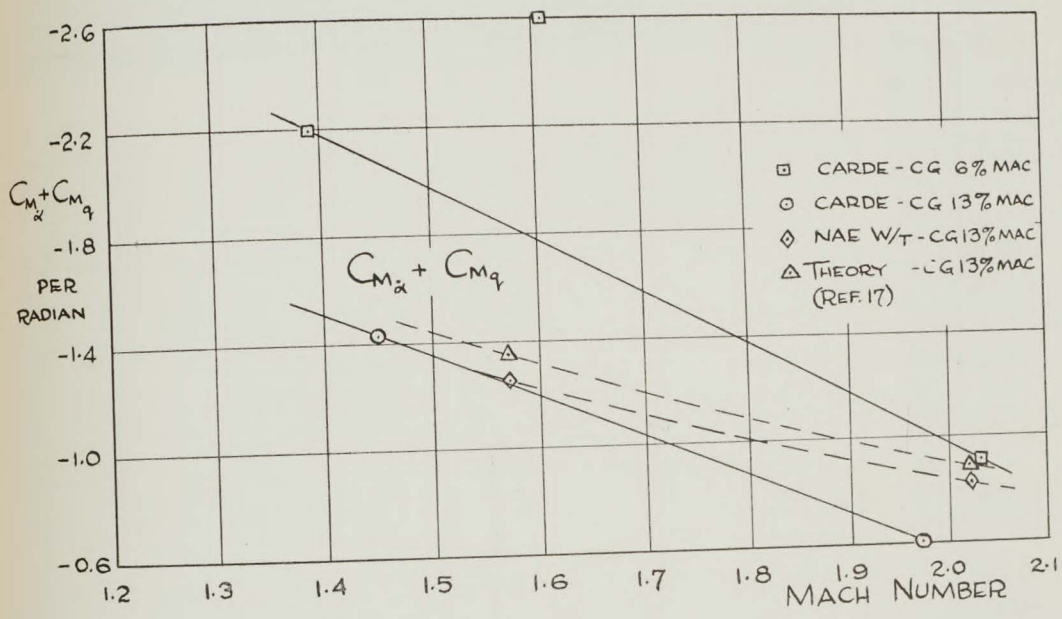

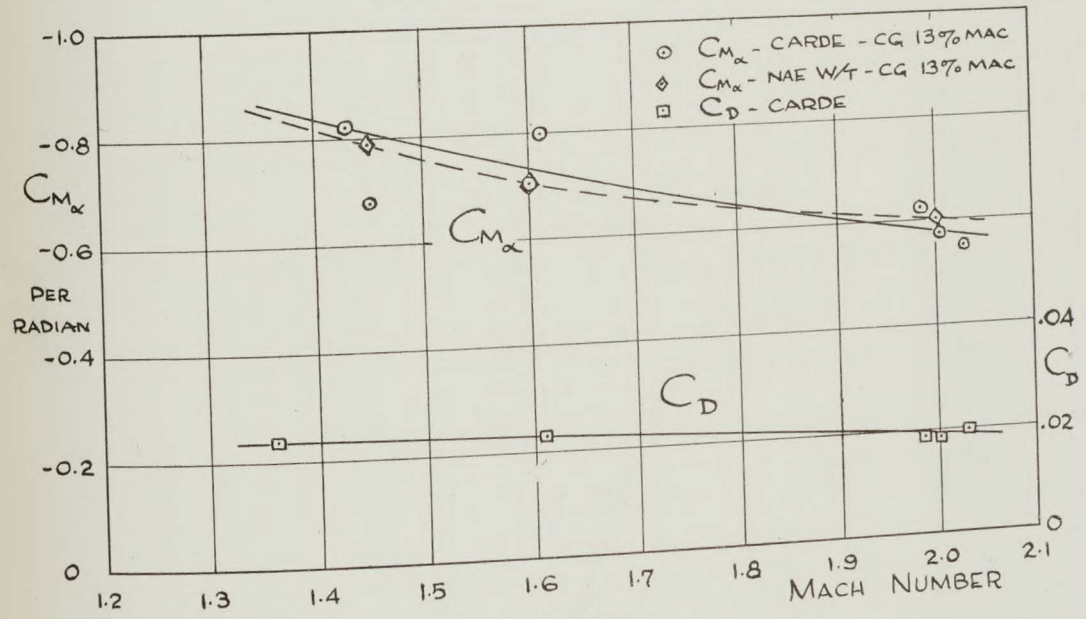

FIGURE 15b
NRC-DELTA LONGITUDINAL DERIVATIVES
(BASED ON MAC)